NF-κB Activation Represses Tumor Necrosis Factor-α-induced Autophagy

Mojgan Djavaheri-Mergny, Manuela Amelotti, Julie Mathieu, Françoise Besançon, Chantal Bauvy, Sylvie Souquère, Gérard Pierron, Patrice Codogno

THE JOURNAL OF BIOLOGICAL CHEMISTRY VOL. 281, NO. 41, pp. 30373–30382, October 13, 2006

NF-κB Activation Represses Tumor Necrosis Factor-α-induced Autophagy*

Received for publication, March 6, 2006, and in revised form, July 17, 2006 Published, JBC Papers in Press, July 20, 2006, DOI 10.1074/jbc.M602097200

Mojgan Djavaheri-Mergny[‡1], Manuela Amelotti[‡§2], Julie Mathieu[¶], Françoise Besançon[¶], Chantal Bauvy[‡], Sylvie Souquère[‖], Gérard Pierron[‖], and Patrice Codogno[‡]

From the [‡]INSERM U756, Faculté de Pharmacie, Université Paris-Sud 11, 5 Rue Jean-Baptiste Clément, 92296 Châtenay-Malabry, France, [§]Laboratory of Biochemistry and Molecular Biology, San Paolo Medical School, Via A. di Rudinì 8, 20142 Milan, Italy, [¶]INSERM U685, Centre Hayem, Hôpital Saint-Louis, 1 Avenue Claude Vellefaux, 75475 Paris Cedex 10, France, and [‖]CNRS-UPR-1983, Institut André Lwoff, Laboratoire de Réplication de l'ADN et Ultrastructure du Noyau, 7 Rue Guy Moquet, 94801 Villejuif, France

Activation of NF-κB and autophagy are two processes involved in the regulation of cell death, but the possible cross-talk between these two signaling pathways is largely unknown. Here, we show that NF-κB activation mediates repression of autophagy in tumor necrosis factor-α (TNFα)-treated Ewing sarcoma cells. This repression is associated with an NF-κB-dependent activation of the autophagy inhibitor mTOR. In contrast, in cells lacking NF-κB activation, TNFα treatment up-regulates the expression of the autophagy-promoting protein Beclin 1 and subsequently induces the accumulation of autophagic vacuoles. Both of these responses are dependent on reactive oxygen species (ROS) production and can be mimicked in NF-κB-competent cells by the addition of H_2O_2. Small interfering RNA-mediated knockdown of *beclin 1* and *atg7* expression, two autophagy-related genes, reduced TNFα- and reactive oxygen species-induced apoptosis in cells lacking NF-κB activation and in NF-κB-competent cells, respectively. These findings demonstrate that autophagy may amplify apoptosis when associated with a death signaling pathway. They are also evidence that inhibition of autophagy is a novel mechanism of the antiapoptotic function of NF-κB activation. We suggest that stimulation of autophagy may be a potential way bypassing the resistance of cancer cells to anti-cancer agents that activate NF-κB.

Acquisition of drug resistance in cancer cells is the major cause of the inefficacy of cancer therapy. Activation of the NF-κB[3] transcription factor is one of the signaling pathways that contributes to the resistance of cancer cells to radio- and chemotherapies (1–4). Indeed, inactivation of NF-κB sensitizes numerous cancer cell lines to the cytotoxic effect of anti-cancer treatments (1–4).

NF-κB is an ubiquitously expressed family of Rel-related transcription factors (5). Typically, in unstimulated cells, NF-κB is sequestered in the cytoplasm by binding to inhibitory κB proteins (IκB). In response to a variety of stimuli, such as inflammatory cytokines, oncogenes, and viruses, the proteasome-dependent degradation of IκB allows the translocation of NF-κB to the nucleus and its binding to the promoter region of target genes involved in the control of different cellular responses, including apoptosis (6–8). In many cancer cells, the constitutive activation of NF-κB activity lowers cell sensitivity to apoptosis and consequently favors neoplastic cell survival (9). Several anti-tumor drugs appear to enhance NF-κB activity, which renders them less effective (10).

Recently, evidence has emerged that autophagy is another mechanism involved in the control of death in cancer cells (11, 12). Macroautophagy (hereafter referred to as autophagy) is a vacuolar lysosomal degradation pathway for organelles and cytoplasmic macromolecules (13, 14). Genetic studies of autophagy in the yeast *Saccharomyces cerevisiae* have led to the identification of a family of genes named *ATG* (autophagy-related gene) involved in the control of autophagy (15–17). The formation of autophagosomes requires two conjugation systems (Atg5–Atg12 and Atg8 lipidation) (18) and a class III phosphatidylinositol 3-kinase (19). This kinase interacts with the tumor suppressor protein Beclin 1, the mammalian orthologue of the yeast Atg 6 (20).

The relation between autophagy and cell death is complex, since autophagy can be involved in either cell death or survival depending on the cellular context (12, 21, 22). The survival function of autophagy has been demonstrated under different physiological situations, such as interruption of maternal nutrient supply in newborn mice (23) or cell deprivation of growth factors and of nutrients (24, 25). Autophagy is also implicated in the cell death process during development (26) and in response to several cytotoxic stimuli (reviewed in Ref. 27). In some situations, both apoptosis and autophagy can occur concomitantly in the same cells, suggesting the involvement of common regulatory mechanisms (28). In fact, several members of both extrinsic (29, 30) and intrinsic (31) apoptotic pathways can promote activation of autophagy. In particular, death receptor

* This work was supported by institutional funding from INSERM and from University Paris-Sud 11. The costs of publication of this article were defrayed in part by the payment of page charges. This article must therefore be hereby marked "*advertisement*" in accordance with 18 U.S.C. Section 1734 solely to indicate this fact.

The nucleotide sequence(s) reported in this paper has been submitted to the GenBank™/EBI Data Bank with accession number(s) NM003766 and BC016045.

[1] To whom correspondence should be addressed: INSERM U756, Faculté de Pharmacie, Université Paris-Sud 11, 5, Rue Jean-Baptiste Clément, 92296 Châtenay-Malabry, France. Tel.: 33-1-46-83-55-28; Fax: 33-1-46-83-58-44; E-mail: mojgan.mergny@cep.u-psud.fr.

[2] Supported by a Ministero dell'Istruzione dell'Università e della Ricerca fellowship.

[3] The abbreviations used are: NF-κB, nuclear factor-κB; IκB, inhibitor κB; PARP, poly(ADP-ribose) polymerase; ROS, reactive oxygen species; TNFα, tumor necrosis factor-α; 4E-BP1, eIF4E-binding protein-1; mTOR, mammalian target of rapamycin; BHA, butylated hydroxyanisole; BNP, *N*-butyl-α-phenylnitrone; MDC, monodansylcadaverine; siRNA, small interfering RNA; 3-MA, 3-methyladenine; Z-VAD-fmk, benzyloxycarbonyl-Val-Ala-Asp(Ome)-fluoromethyl ketone.

ligands, such as TNFα (30) and Trail (TNF-related apoptosis-inducing ligand) (29), stimulate autophagy in T-lymphoblastic cells and in a model of lumen formation in mammary acini, respectively. In addition, some participants in apoptosis signaling, such as the receptor-interacting proteins RIP (32) and FADD (Fas-associated death domain protein) (33), and the kinase c-Jun N-terminal kinase (32), have recently been implicated in autophagy. The precise network that controls the cross-talk between apoptosis and autophagy remains to be elucidated. In particular, it has not yet been investigated whether NF-κB, one of the major regulators of apoptosis, also controls autophagy.

Here, we examined whether NF-κB activation modulates the autophagic capacity of cells. We compared the autophagic capacity of NF-κB competent cells with that of cells carrying a repressor of NF-κB activation after treatment with TNFα. We found that whereas TNFα induced autophagy in cells lacking NF-κB activity, it did not activate this process in NF-κB-competent cells. We also demonstrate that in the absence of NF-κB activation, TNFα-induced autophagy is dependent on ROS production and participates in the TNFα-induced apoptotic signaling pathway.

EXPERIMENTAL PROCEDURES

Reagents—Hoechst 33258 dye, benzon nuclease, 3-methyladenine, monodansylcadaverine (MDC), hydrogen peroxide, butylated hydroxyanisole (BHA), and *N*-butyl-α-phenyl-nitrone (BNP) were from Sigma. L-[^{14}C]valine (5.47 GBq/mmol) was from PerkinElmer Life Sciences. Z-VAD-fmk and recombinant human TNFα (TNFα was used in cells at a concentration of 2000 units/ml) were from R&D Systems, Inc. (Minneapolis, MN). Antibodies against the following proteins were used: Atg5 (Santa Cruz Biotechnology, Inc., Santa Cruz, CA), Atg 7 (kindly provided by Dr. W. A. Dunn, Jr., University of Florida College of Medicine, Gainesville, FL), Beclin 1 and actin (BD Biosciences), phospho-4-EBP1, 4-EBP1, phospho-p70 S6 kinase, p70 S6 kinase, Bcl-2 (Cell Signaling Technology, Inc.) LC3 (kindly provided by Dr. Eiki Kominami (Jutendo University, Tokyo, Japan) and Dr. Tamotsu Yoshimori, National Institute of Genetics (Mishima, Japan)), and PARP (Alexis, Illkirch, France).

Cells—EW7 cells transfected with an empty pcDNA vector (EW7PC cells) or with the IκBα (A32/36)-encoding vector (EW7MAD cells) were previously described (34). The generation of promyelocytic leukemia cells (NB4) expressing either the Migr-eGFP vector (NB4/GFP cells) or the IκBα (A32/36)-encoding Migr-eGFP (NB4/GFP-MAD) was previously described (35). All of these cells were grown at 37 °C in 5% CO_2 RPMI medium supplemented with 2 mM L-glutamine and 10% decomplemented fetal calf serum. The human breast cancer MCF7 cell line (from ATCC) were grown at 37 °C in 10% CO_2 in Dulbecco's modified Eagle's medium supplemented with 10% decomplemented fetal calf serum.

Monodansylcadaverine Staining—MDC was used to evaluate the abundance of autophagic vacuoles in cells as previously reported (36). A 10 mM stock solution of MDC was prepared in Me_2SO. Following treatment, cells were stained with MDC at a final concentration of 10 μM, for 10 min at 37 °C, and then collected and fixed using 3% paraformaldehyde solution in phosphate-buffered saline for 30 min. Cells were washed and then examined by fluorescence microscopy (Zeiss Axioplan microscope). For each condition, the percentage of cells with characteristic MDC staining dots indicative of autophagy was assessed.

Analysis of Degradation of Long Lived Proteins—Ewing sarcoma-derived cell lines were incubated with 0.2 μCi/ml [^{14}C]L-valine in complete medium (RPMI medium supplemented with 2 mM L-glutamine and 10% fetal calf serum) for 24 h at 37 °C (37). At the end of the radiolabeling period, unincorporated radioisotopes were removed by washing the cells three times with phosphate-buffered saline (pH 7.4). Cells were then incubated in complete medium supplemented with 10 mM unlabeled valine for 1 h (prechase period). After this time, the medium was replaced by either nutrient-free medium (Hanks' balanced salt solution plus 0.1% bovine serum albumin) or complete medium plus 10 mM unlabeled valine in the presence and absence of 10 mM 3-MA and TNFα for a 4–8-h incubation (chase period). Radiolabeled proteins from the medium and adherent cells were precipitated in trichloroacetic acid at the final concentration of 10% (v/v), separated from soluble radioactivity by centrifugation at 600 × *g* for 20 min, and dissolved in 1 ml of 0.2 N NaOH. The rate of protein degradation was calculated by determining the ratio of radioactivity in acid-soluble proteins obtained from cells and medium to radioactivity in trichloroacetic acid-precipitated proteins obtained from cells and medium.

Electron Microscopy—Cells were fixed for 1 h at 4 °C in 1.6% glutaraldehyde in 0.1 M Sörensen phosphate buffer (pH 7.3), washed, and fixed again in aqueous 2% osmium tetroxide, dehydrated in ethanol, embedded in Epon, and processed for electron microscopy with a Zeiss EM 902 transmission electron microscope at 80 kV, in ultrathin sections stained with uranyl acetate and lead citrate.

Detection of Apoptosis—Apoptotic cell death was determined by quantification of apoptotic nuclei (*i.e.* fragmentation and condensation of nuclei) following Hoechst 33258 staining. A total of 500 nuclei were counted for each sample. Apoptosis was also evaluated by determination of caspase 3 activity, which was assessed by the appearance of PARP1 cleaved product revealed by Western blotting analysis. DNA fragmentation was quantified using a cell death detection ELISA Plus kit (Roche Applied Science), which was used according to the manufacturer's instructions.

Isolation of RNA and Real Time Quantitative Reverse Transcription-PCR—Total RNA was extracted with the RNeasy Mini kit (Qiagen, Courtaboeuf, France). First-strand cDNA was generated by reverse transcription of 2 μg of total RNA using random primers and Superscript™III reverse transcriptase (Invitrogen) according to the manufacturer's instructions, in a total reaction volume of 20 μl. The sequences of forward and reverse oligonucleotide primers, specific to the chosen candidate and housekeeping genes, were designed using Primer3 software (available on the World Wide Web at frodo.wi.mit.edu/cgi-bin/primer3/primer3_www.cgi). The primers are for Beclin 1 (forward, 5′-GGCTGAGAGACTGGATCAGG-3′; reverse, 5′-CTGCGTC-

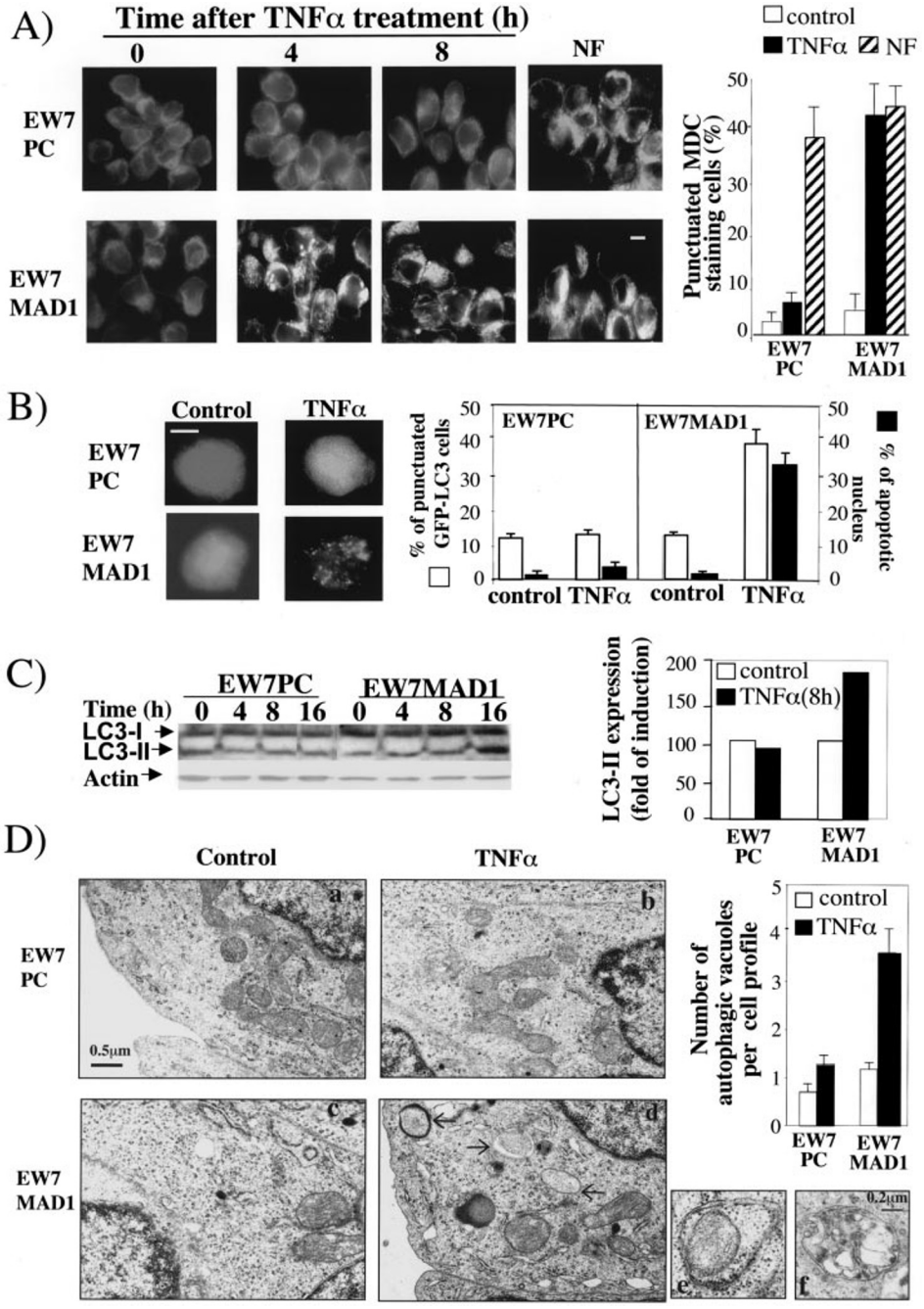

FIGURE 1. **TNFα stimulates autophagy in Ewing sarcoma cells expressing a repressor of NF-κB activation.** *A*, EW7PC and EW7MAD1 cells were treated with TNFα (2000 units/ml) for different times or were incubated for 4 h in nutrient-free medium (*NF*). Cells were stained with MDC as detailed under "Experimental Procedures." *Left*, representative images of three independent experiments. *Bar*, 6 μm. *Right*, the percentage of cells with MDC staining dots per total MDC staining cells was quantified after treatment with either TNFα (8 h) or nutrient-free medium treatment 4 h.. Values reported are the mean ± S.D. of three independent experiments. *B*, *left*, representative images of GFP-LC3 staining in EW7PC and EW7MAD1 cells incubated for 8 h in the presence and absence of TNFα. *Bar*, 3 μm. *Right*, the percentage of cells with punctated GFP-LC3 per total GFP-LC3 cells was scored. Values are the mean ± S.D. of three independent experiments. For each condition, cells are also subjected to Hoechst staining, and the percentage of apoptotic nuclei was scored. *C*, *left*, immunoblot analysis of LC3-I processing into LC3-II in EW7PC and EW7MAD1 cells treated with TNFα for the indicated times. *Right*, bands corresponding to LC3-II (at time point 8 h) were quantified using NIH Image software and were normalized to actin expression level. *D*, *left*, *a–d*, representative electron micrographs of EW7PC and EW7MAD1 cells treated for 4 h in the presence and absence of TNFα are shown. The *arrowheads* denote the presence of autophagic vacuoles. *Bar*, 0.5 μm. *e* and *f*, higher magnifications of TNFα-treated EW7MAD1 cells show autophagosomes containing mitochondrion (*e*) or digested cytoplasmic materials (*f*). The *bar* represents 0.2 μm. *Right,* the total number of autophagic vacuoles per cell profile was determined for each condition. Results shown in *D* are the mean ± S.D. of five profiles for each condition.

TGGGCATAACG-3′; GenBank™ NM003766; nucleotides 787–913) and β-actin (forward, 5′-TCACCCACACTGTGCCCATCTACGA-3′; reverse, 5′-CAGCGGAACCGCTCATTGCCAATGG-3′; GenBank™ BC016045; nucleotides 555–845).

Real time quantitative PCR was performed in a LightCycler® (Roche Applied Science) thermal cycler. An 80-fold dilution of each cDNA was amplified in a 10-μl volume, using the Fast Start DNA Master^{PLUS} SYBR Green I master mix (Roche Applied Science), with 500 nM final concentrations of each primer. The amplification specificity was checked by melting curve analysis and gel-agarose electrophoresis of PCR products. Threshold cycle Ct, which correlates inversely with the target mRNA levels, was calculated using the second derivative maximum algorithm provided by the LightCycler software. For each cDNA, the Beclin 1 mRNA levels were normalized to β-actin mRNA levels. Results are expressed as ratio of normalized Beclin 1 mRNA level of treated cells to those of untreated cells.

Transfection and RNA Interference—Small interfering RNAs (siRNAs) against *beclin 1*, *atg7*, and *p65* and control siRNA were synthesized by Eurogentec (Seraing, Belgium). The siRNA sequences against *beclin-1*, *atg7*, and *p65* were previously described in Refs. 25, 38, and 39, respectively. Cells cultured in 6-well plates were transfected with siRNA at 200 nM final concentration by using oligofectamine reagent (Invitrogen). Cells were then incubated for 8 h at 37 °C prior to the addition of 5% fetal calf serum and then left for another 48–92 h. At the end of these treatments, cells were harvested and subjected to Western blotting analysis or apoptosis assays.

Transient transfections with GFP-LC3 plasmids (kindly provided by Dr. Tamotsu Yoshimori, National Institute of Genetics, Mishima, Japan) were carried out by using Lipofectamine 2000 transfection reagent according to

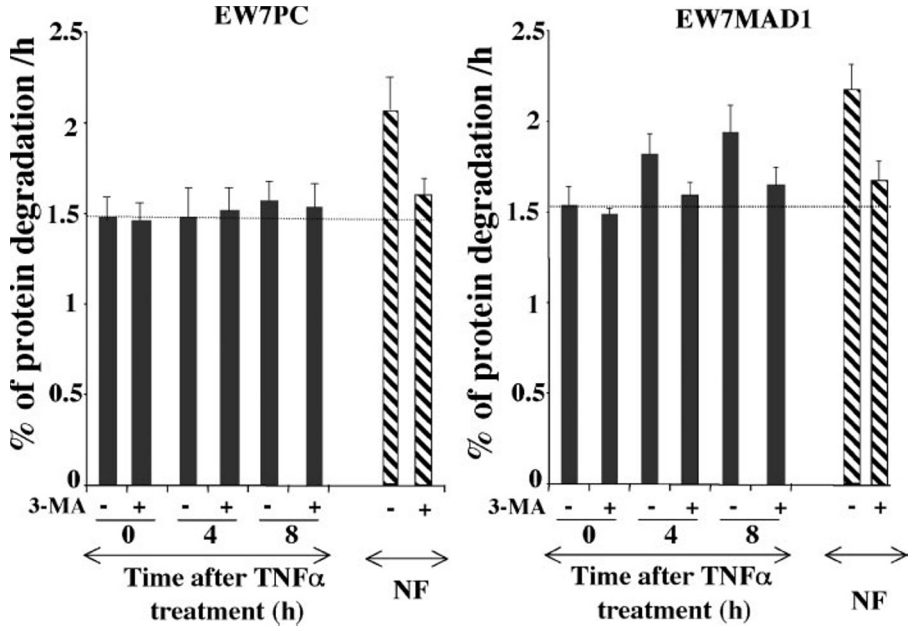

FIGURE 2. **The effect of TNFα on long lived protein degradation in EW7PC and EW7MAD1 cells.** The rate of proteolysis of [^{14}C]valine-labeled long lived proteins was measured in cells following an 8-h incubation with TNFα in the presence and absence of 10 mM 3-MA. As a positive control, cells were subjected to 4-h starvation in the presence and absence of 10 mM 3-MA. Results are the mean ± S.D. of three independent experiments.

the manufacturer's instructions. Since the level of transfection in Ewing sarcoma cells only reaches 15% of the total amount of cells, 2×10^6 cells were transfected for each assay and then subjected to fluorescence microscopy analysis. For each condition, at least 150 GFP-LC3-transfected cells (GFP-expressing cells) were observed, and the percentage of transfected cells presenting punctate GFP-LC3 staining, which is indicative of autophagy structures, was determined.

Western Blot Analysis—Cellular extracts were prepared in 10 mM Tris, pH 7.4, 1% SDS, 1 mM sodium vanadate, treated with benzon nuclease for 5 min at room temperature, and boiled for 3 min. Fractions (30 μg) of cellular extract proteins were subjected to SDS-polyacrylamide gel electrophoresis using a Tris/glycine buffer system based on the method of Laemmli. After electrophoresis, proteins were transferred to a Protean nitrocellulose transfer membrane (Amersham Biosciences). Protein loading was assessed by Ponceau staining of membranes. Blots were then incubated with primary antibodies using the manufacturer's protocol followed by the appropriate horseradish peroxidase-conjugated secondary antibody. Immunostained proteins were visualized on x-ray film using the ECL detection system (Amersham Biosciences). The experiments were repeated at least three times, and representative autoradiograms are shown.

RESULTS

Inhibition of NF-κB Activation Triggers Autophagy in TNFα-treated Ewing Sarcoma Cells—To evaluate the relation between NF-κB activation status and autophagy, we compared the autophagic activity after TNFα treatment in cells lacking NF-κB activity (EW7MAD1) and NF-κB-competent (EW7PC) Ewing sarcoma cells. The formation of autophagic vacuoles was first assessed by staining with MDC, which accumulates in acidic cell compartments enriched in lipids (36). This leads to a punctate staining pattern when autophagy is stimulated (36). As shown in Fig. 1*A*, both control cells (EW7PC) and cells expressing the repressor of NF-κB activation (EW7MAD1) presented diffuse staining in the absence of TNFα. TNFα treatment of cells lacking NF-κB activity resulted in the appearance of punctate structures 4 h after treatment. In addition, the number and size of these punctate structures were significantly increased following 8 h of TNFα treatment, suggesting that TNFα induces the accumulation of autophagic vacuoles in these cells. Conversely, the accumulation of autophagic vacuoles by TNFα is impaired in NF-κB-competent cells (EW7PC), as revealed by the paucity of punctate structures observed in these cells. To verify that EW7PC cells are not defective in stimulation of autophagic activity, MDC staining was also performed following incubation of these cells in nutrient-free medium, a condition known to stimulate autophagy (14). Under these conditions, EW7PC cells as well as EW7MAD1 cells were both able to induce autophagy (Fig. 1*A*). The redistribution of LC3 from diffuse cytosolic staining to punctate staining is a reliable marker of autophagosome formation (40). This can be examined either by transfection of cells using GFP-LC3 expression plasmids, which result in the formation of punctate fluorescence structures in conditions of autophagy stimulation, or by examining the appearance of the phosphatidylethanolamine-conjugated form of LC3 (LC3-II), which is associated with autophagosomal membranes. After cell transfection with GFP-LC3, TNFα caused the appearance of a punctate fluorescence pattern in EW7MAD1 but not in EW7PC cells (Fig. 1*B*), confirming again that TNFα induces an increase in autophagic structures only in the absence of NF-κB activation. Accordingly, TNFα induces a time-dependent accumulation of the LC3-II form in EW7MAD1 cells (Fig. 1*C*), whereas the level of LC3 II was not significantly modified in TNFα-treated EW7PC cells as compared with untreated cells. Interestingly, accumulation of autophagic vacuoles in TNFα-treated cells lacking NF-κB activity correlated with their susceptibility to apoptosis (Fig. 1*B*, *right*). Transmission electron microscopy experiments were also used to visualize autophagic vacuoles in cells (Fig. 1*D*, *a–d*). Quantitation of electron micrographs reveals an increase in the number of autophagic vacuoles after 4-h TNFα treatment of cells lacking NF-κB activity as compared with EW7PC cells. The presence of autophagosomes containing mitochondrion (Fig. 1*D*, *e*) and degraded cytoplasmic materials was confirmed by electron microscopy (Fig. 1*D*, *f*).

To verify that the increase in the number of autophagic vacuoles in TNFα-treated EW7MAD1 cells represents an activation of autophagic activity rather than inhibition of autophagic vacuoles/lysosome fusion, we further measured the degrada-

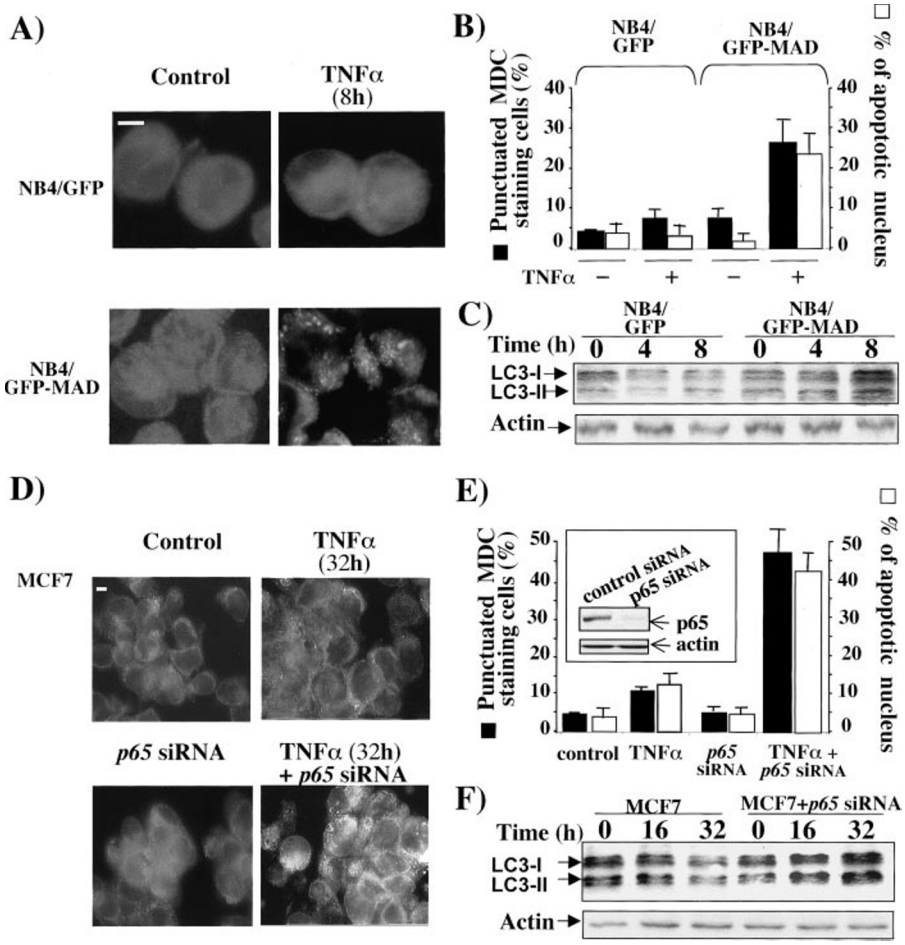

FIGURE 3. **Inactivation of NF-κB in NB4 and MCF7 cells induces autophagy in response to TNFα.** NF-κB-competent NB4 cells (NB4/GFP), NB4 cells expressing an inhibitor of NF-κB activation (NB4/GFP-MAD), MCF7 cells, and MCF7 cells transiently transfected with siRNA against p65 were treated with TNFα (2000 units/ml) for different times as indicated. *A* and *D*, representative control cells and TNFα-treated cells labeled with MDC are shown. *Bar*, 3 μm. *B* and *E*, the percentage of cells with MDC-stained dots was quantified after treatment with TNFα of NB4 cells or MCF7 cells, for 8 or 32 h, respectively (*black bar*). *Inset*, the levels of p65 protein expression in the presence and absence of p65 siRNA are shown. For each condition, cells were also subjected to Hoechst staining, and the percentage of apoptotic nuclei was scored (*white bar*). *C* and *F*, immunoblot analysis of LC3-I processing into LC3-II in NB4/GFP and NB4/GFPMAD cells treated in the presence and absence of TNFα (*C*) and in MCF7 cells incubated for 32 h with siRNA against p65 before the addition of TNFα (*F*).

tion of long lived proteins in the presence and the absence of the autophagy inhibitor, 3-MA. As shown in Fig. 2, the rate of 3-MA-sensitive proteolysis of long lived proteins was increased in a time-dependent manner after TNFα treatment in EW7MAD1 cells but not in EW7PC cells. Thus, the accumulation of autophagic vacuoles observed in TNFα-treated EW7MAD1 cells results from the activation of autophagy but not from the impairment of lysosomal delivery of LC3-positive vacuoles. It is worth nothing that 3-MA-sensitive proteolysis is increased in both cell lines incubated in nutrient-free medium, confirming again that both cell lines are competent for induction of autophagy.

Overall, these findings demonstrate that inhibition of NF-κB activity results in induction of autophagy in TNFα-treated EW7MAD1 cells. Such autophagic hallmarks were also observed in another clone of Ewing sarcoma cells expressing a repressor of NF-κB activation, EW7MAD2 cells after TNFα treatment (data not shown).

The NF-κB-dependent Repression of Autophagy Occurs Also in NB4 and MCF7 Cells—To investigate whether the NF-κB-dependent regulation of autophagy observed in Ewing sarcoma may extend to other cell lines, we examined the autophagic capacity of two additional cell lines, the promyelocytic leukemia cells (NB4) and the human breast cells (MCF7), in the presence and absence NF-κB activation. Autophagy was evaluated by either MDC staining or detection of the accumulation of the LC3-II form by Western blotting.

We first compared the autophagic activity in TNFα-treated NB4 cells (NB4/GFP) and in TNFα-treated NB4 cells expressing a repressor of NF-κB activation (NB4/GFP-MAD). As shown by MDC staining (Fig. 3*A*), TNFα induced a great accumulation of autophagic vacuoles only in cells lacking NF-κB activity (NB4/GFP-MAD) but not in NB4/GFP. Accordingly, TNFα treatment resulted in an increased level of the LC3-II form only in the absence of NF-κB activation (Fig. 3*C*). As in Ewing sarcoma cells, this accumulation of autophagic vacuoles observed in TNFα-treated NB4/GFP-MAD cells correlated with their susceptibility to apoptosis induced by TNFα (Fig. 3*B*).

We also examined the autophagy capacity of MCF7 cells following siRNA knockdown of p65 protein, a member of the NF-κB complex. The complete reduction of p65 expression by using specific siRNA (39) (Fig. 3*E*, *inset*) sensitized MCF7 cells to TNFα-induced apoptosis (Fig. 3*E*) and triggered accumulation of autophagic vacuoles in these cells as revealed by MDC staining (Fig. 3, *D* and *E*). Accordingly, TNFα induced an accumulation of LC3II form only in MCF7 treated with siRNA against p65 (Fig. 3*F*). Overall, these data indicate that inhibition of NF-κB in both NB4 and MCF7 cells induces autophagy in response to TNFα.

ROS Are Involved in TNFα-induced Autophagy in Cells Lacking NF-κB Activity—We have previously shown that inhibition of NF-κB activity results in an increase in ROS production in TNFα-treated Ewing sarcoma cells (41). We therefore questioned whether TNFα-induced ROS production is involved in stimulation of autophagy. To this aim, we treated EW7MAD1 cells with BHA, a ROS scavenger, prior to the addition of TNFα. Autophagy was evaluated by MDC or GFP-LC3 staining. As shown in Fig. 4*A*, treatment with this antioxidant reduced the

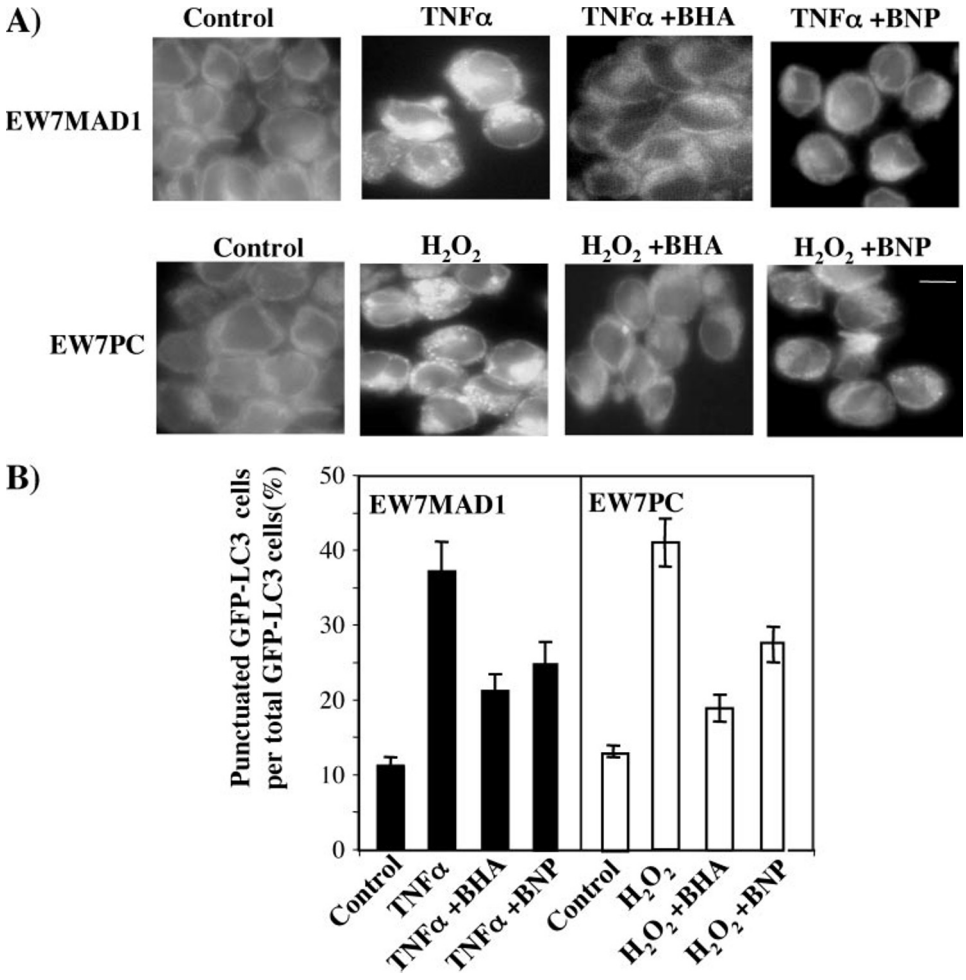

FIGURE 4. **ROS scavengers inhibit TNFα-induced autophagy in EW7MAD1 cells.** EW7MAD1 and EW7PC cells were treated with either BHA (100 μM) or BNP (50 μM) for 2 h prior to treatment with TNFα (2000 units/ml, 8 h) and H_2O_2 (100 μM, 8 h), respectively. *A*, fluorescence microscopy was performed following MDC staining. Representative images of cells with MDC staining are shown. *Bar*, 6 μm. *B*, EW7PC and EW7MAD1 cells were transfected with GFP-LC3 plasmids and then subjected to treatment as indicated in *A*. For each condition, the percentage of cells with punctate GFP-LC3 staining was quantified. Results shown in *A* and *B* are representative of three independent experiments.

accumulation of autophagic vacuoles induced by TNFα in EW7MAD1 cells. Similar results were found by using another ROS scavenger, BNP (Fig. 4*A*). This indicates that the production of ROS is required for the induction of autophagy in TNFα-treated EW7MAD1 cells. To confirm more precisely the role of ROS in induction of autophagy, we further examined the effect of the H_2O_2 addition on the modulation of autophagic activity in NF-κB-competent cells. As revealed by MDC staining, treatment with H_2O_2 induced an accumulation of acidic vacuoles in EW7PC cells. The appearance of autophagic vacuoles was inhibited in the presence of both BHA and BNP (Fig. 4, *A* and *B*). Similar results were found in GFP-LC3-transfected cells, showing that both TNFα and H_2O_2 promote an increase in the number of autophagic structures in EW7MAD1 and EW7PC cells, respectively (Fig. 4*B*). Both responses were reduced in the presence of BHA and BNP, confirming again that the stimulation of autophagy induced either by TNFα or H_2O_2 involves a ROS-dependent mechanism (Fig. 4, *A* and *B*).

Analysis of Autophagy-regulated Protein Expression in TNFα-treated EW7PC Cells and TNFα-treated EW7MAD1 Cells—Autophagy is mediated by Atg proteins (17) and can be negatively regulated by activation of mTOR (42, 43). To gain further insight into the mechanisms of induction of autophagy in cells lacking NF-κB activity, we compared the pattern of activation or expression of such autophagy-regulated proteins in TNFα-treated EW7PC cells and in TNFα-treated EW7MAD1 cells.

We first examined the activity of mTOR by analyzing the phosphorylation of two of its substrates, the p70 protein S6 kinase and the eukaryotic initiation factor 4-E-binding protein 1 (4E-BP1). As shown in Fig. 5*A*, TNFα treatment of EW7PC cells resulted in an increase in the level of phosphorylation of both 4E-BP1 and p70 S6 kinase proteins. In contrast, TNFα treatment of Ewing sarcoma cells lacking NF-κB activity reduced the levels of phospho-4E-BP1 and did not significantly change the level of phospho-p70 S6 kinase. These results indicate that TNFα induced repression of mTOR activation only when NF-κB activity was inhibited, which is in accordance with the results showing that TNFα induces autophagy in EW7MAD1 cells but not in EW7PC control cells.

We further examined the expression patterns of Atg7, Atg5, and Beclin 1, three Atg proteins involved in autophagosome formation (17), and of Bcl-2, an antiapoptotic protein that negatively regulates autophagy through its interaction with Beclin 1 (44). As shown in Fig. 5*A*, TNFα caused a strong decrease in the level of Bcl-2 protein in EW7MAD1 cells but not in EW7PC cells. Furthermore, whereas the expression level of Beclin 1 remained unchanged following TNFα treatment of EW7PC, it was up-regulated in EW7MAD1 cells 4 h after TNFα addition. The levels of expression of Atg7 and Atg5 were not modified upon TNFα treatment of both cell lines. To further specify the time course of the modulation of Beclin 1 expression by TNFα, we also examined the expression level of Beclin 1 upon short times of incubation with TNFα in both cell lines. We found that TNFα induces a rapid increase in Beclin 1 expression level in EW7MAD1 cells 0.5 h after treatment (Fig. 5*B*). Interestingly, the level of Beclin 1 expression was unchanged during the time course of TNFα treatment of EW7PC cells. To investigate whether the TNFα-induced accumulation of Beclin 1 expression is dependent on the increased transcription of the *beclin 1* gene or stabilization of its protein, we examined the expression of mRNA level of Beclin 1 by performing real time quantitative

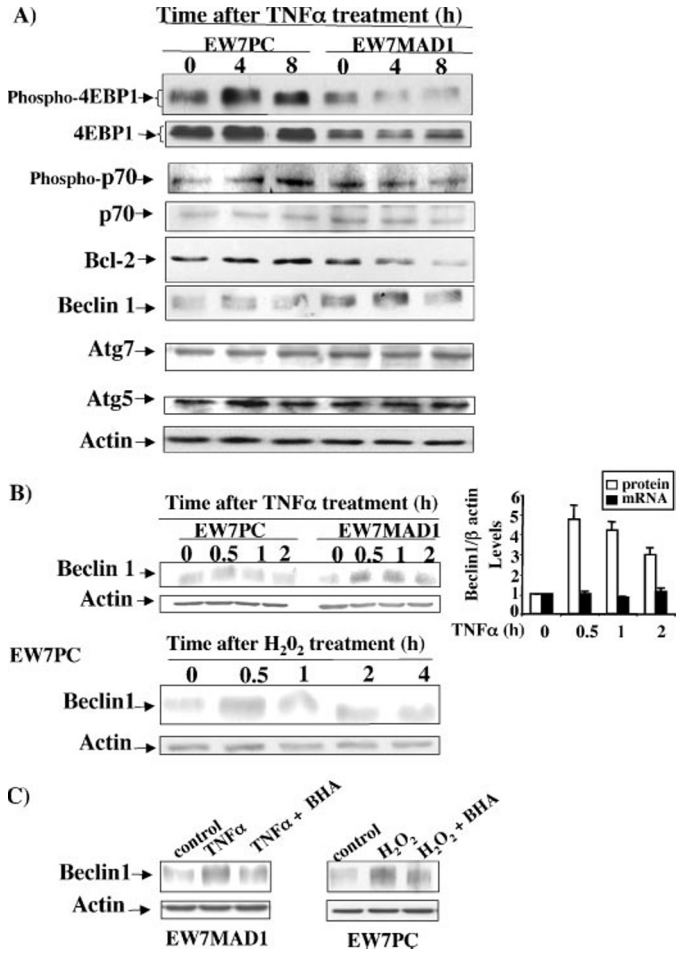

FIGURE 5. **Comparison of autophagy-regulated protein expression in TNFα-treated EW7PC cells and in TNFα-treated EW7MAD cells.** *A*, EW7PC and EW7MAD1 cells were treated for the indicated times with TNFα before cell lysis. Equal protein amounts of whole cell extracts were analyzed by Western blotting using antibodies directed against phospho-4E-BP1, 4E-BP1, phospho-p70 S6 kinase, p70 S6 kinase, Beclin 1, Atg7 and Atg5, Bcl-2, and actin. *B*, EW7PC and EW7MAD1 cells were treated for the indicated times with either TNFα (2000 units/ml) or H_2O_2 (100 μM). *Left*, cellular extracts were prepared and analyzed for the expression level of Beclin 1. The bands corresponding to the Beclin 1 protein level in EW7MAD1 cells were quantified using NIH Image software and were normalized to actin expression level (*right*). *Right*, total RNA was extracted from TNFα-treated EW7MAD1 cells before the measurement of the Beclin 1 mRNA level by real time quantitative reverse transcription-PCR. Values obtained for Beclin 1 mRNA transcripts were normalized to those of β-actin. *C*, EW7MAD1 and EW7PC cells were first treated with BHA (100 μM) and then incubated with TNFα (2000 units/ml, 1 h) or H_2O_2 (100 μM, 0.5 h), respectively. Cellular extracts were prepared and analyzed for Beclin 1 expression by Western blotting. Results shown in *A–C* are representative of three independent experiments.

reverse transcription-PCR. As shown in Fig. 5*B* (*right*), the level of Beclin 1 mRNA was not significantly modified during 2-h treatment with TNFα of EW7MAD1 cells, suggesting that the increase of Beclin 1 protein expression in TNFα-treated EW7MAD1 cells results from a stabilization of the protein rather than from an increase in mRNA levels. In the same way, we found that the addition of H_2O_2 rapidly increased the expression of Beclin 1 protein in EW7PC NF-κB-competent cells (Fig. 6*B*). To investigate whether these accumulations of Beclin 1 protein are dependent on ROS production, we examined the effect of antioxidant. As shown in Fig. 5*C* (*left*), pretreatment of EW7MAD1 cells with BHA markedly prevented TNFα-induced Beclin 1 expression protein. Similarly, H_2O_2-induced up-regulation of Beclin 1 protein was reduced by the addition of BHA (Fig. 5*C*, *right*). Collectively, these data show that both TNFα and H_2O_2 cause a rapid ROS-dependent increase in Beclin 1 expression prior to the accumulation of autophagic vacuoles.

Activation of Autophagy Participates in the Apoptotic Signaling Triggered by TNFα in EW7MAD1 Cells—To investigate the role of autophagy in TNFα-induced apoptosis in EW7MAD1 cells, we knocked down the expression of *beclin 1* and *Atg7* by using specific siRNAs. As shown in Fig. 6*A*, these treatments resulted in an inhibition of TNFα-induced autophagy in EW7MAD1 cells. Apoptosis was evaluated by Hoechst staining, detection of the cleaved form of PARP1, and quantification of nucleosomal DNA fragmentation in cells. As shown in Fig. 6*B*, the inhibition of both *beclin 1* and *atg7* expression by specific siRNA reduced the accumulation of apoptotic nuclei (condensed and fragmented nuclei) in TNFα-treated EW7MAD1 cells (Fig. 6*B*, *left* and *right*). Furthermore, TNFα-mediated PARP1 cleavage in TNFα-treated EW7MAD1 was reduced after knockdown of *beclin 1* and *atg7* (Fig. 6*C*, *left*). Apoptosis was also quantified by using a DNA fragmentation enzyme-linked immunosorbent assay. As shown in Fig. 6*C* (*right*), TNFα-induced nucleosomal DNA fragmentation in EW7MAD1 was markedly decreased following inhibition of autophagy by using *beclin 1* and *atg7* siRNAs.

Altogether, these findings show that inhibition of autophagy reduces TNFα-induced apoptosis in EW7MAD1 cells, suggesting that autophagy is involved in the apoptotic pathway under these conditions. Similarly, H_2O_2-induced apoptosis in EW7PC cells was reduced following inhibition of autophagy by using siRNA directed against *beclin 1* and *atg7*, indicating that autophagy is also implicated in the signaling pathway leading to ROS-induced apoptosis (Fig. 6*D*). Interestingly, inhibition of autophagy by using specific siRNA also reduced TNFα-induced ROS production in EW7MAD1 cells (data not shown). These observations are in accordance with a previous report supporting that autophagy contributes in the regulation of cellular ROS production (45).

Caspase Activation Inhibits TNFα-induced Autophagy in EW7MAD1 Cells—Since the treatment of EW7MAD1 cells with TNFα elicits caspase-dependent cell death (34, 41), we further examined whether caspases modulate TNFα-induced autophagy. We treated cells with Z-VAD-fmk, a broad spectrum caspase inhibitor, prior to the addition of TNFα. Autophagy was evaluated by either MDC staining or detection of the accumulation of the LC3-II form by Western blotting. As previously shown (34), Z-VAD-fmk completely inhibited TNFα-induced apoptosis in these cells (data not shown). As shown by MDC staining, the addition of Z-VAD-fmk prior to TNFα treatment increased the number and size of autophagic vacuoles as compared with TNFα alone (Fig. 7*A*). Similarly, the accumulation of the LC3-II form induced by TNFα was enhanced following the addition of Z-VAD-fmk (Fig. 7*B*). These results indicate that caspase activation down-regulates autophagy.

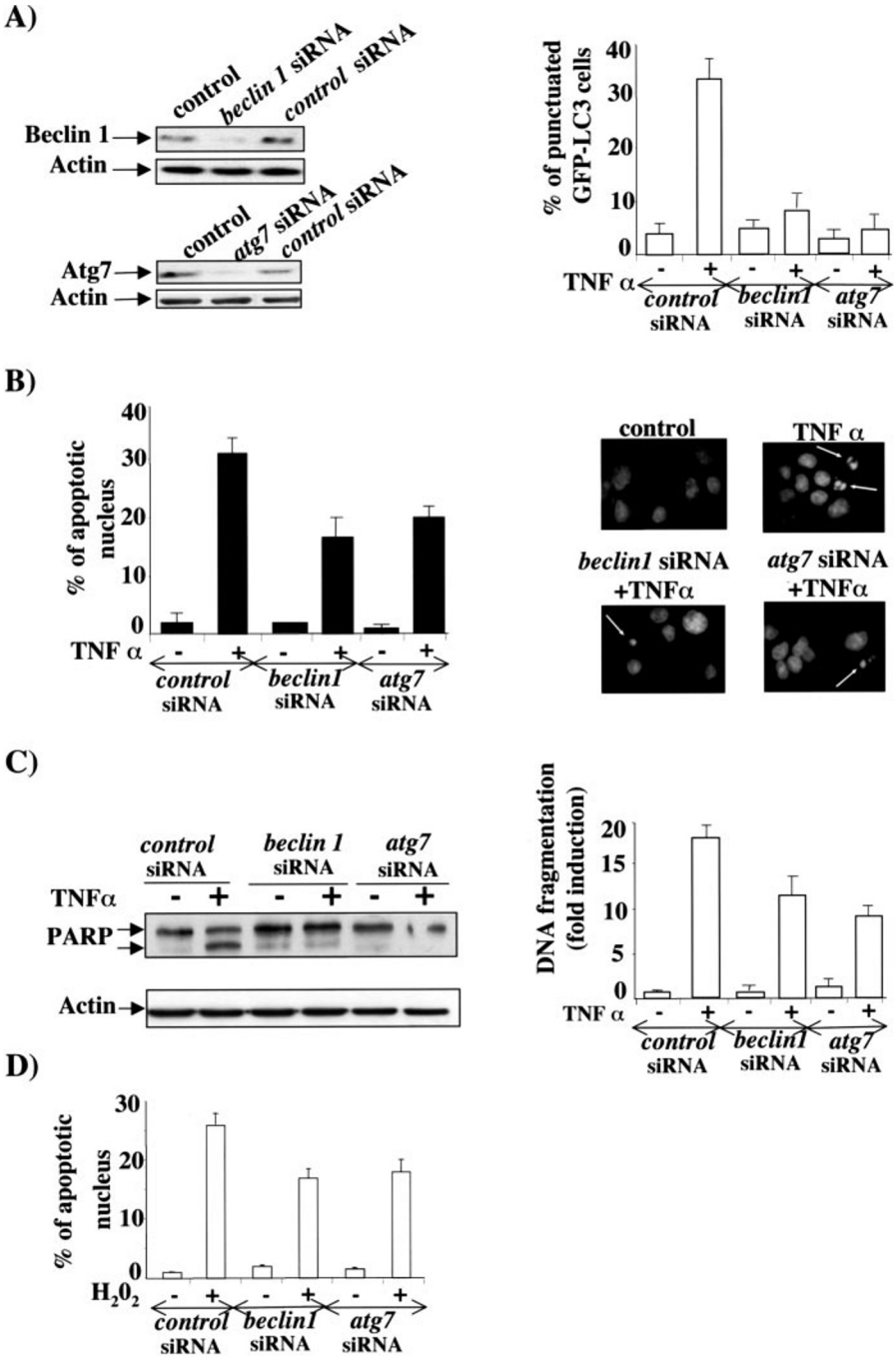

FIGURE 6. **Effect of autophagy inhibition on TNFα-induced apoptosis in EW7MAD1 cells.** EW7MAD1 cells were transiently transfected with *beclin 1* siRNA, *atg7* siRNA, or control siRNA. TNFα (2000 units/ml, 8 h) was added 54 h later. *A*, *left*, cell extracts were analyzed by Western blotting using antibodies against Beclin 1, Atg7. *Right*, the percentage of cells with punctated GFP-LC3 per total GFP-LC3 cells was scored. Values are the mean ± S.D. of two independent experiments. *B*, *left*, the percentage of cells carrying an apoptotic nuclei was determined by Hoechst staining. Values are the mean ± S.D. of four independent experiments. *Right*, representative cells are shown, and the *arrowheads* indicate apoptotic nuclei (condensed and fragmented nuclei). *C*, *left*, cellular extracts were analyzed by Western blotting using antibodies against PARP1 and actin. *Right*, apoptosis was measured by quantification of nucleosomal DNA fragmentation. The ratio of DNA fragmentation in TNFα-treated cells to that in untreated cells was determined. Results are representative of three independent experiments. *D*, EW7PC cells were transiently transfected with *beclin 1* siRNA, *atg7* siRNA, or *control* siRNA. H_2O_2 (100 μM, 8 h) was added 54 h after transfection. The percentage of cells carrying an apoptotic nucleus was determined by Hoescht staining.

DISCUSSION

NF-κB is most commonly considered as a mediator of tumor promotion based on its ability to promote cell survival, enhance cell proliferation, and decrease the sensitivity of cancer cells to apoptosis (1, 2, 10, 46). Studies focused on identifying the mechanisms involved in the antiapoptotic functions of NF-κB (46) have demonstrated that its activation results in an increased expression of several antiapoptotic proteins, such as Bcl-2 family members (6, 47) or caspase-inhibitory proteins (7). Another antiapoptotic mechanism associated with the activation of NF-κB involves the impairment of both prolonged activation of c-Jun N-terminal kinase (41, 48, 49) and ROS production through up-regulation of antioxidant proteins (41, 50–53).

The present study uncovers a novel antiapoptotic function of NF-κB activation that consists in repression of autophagy. We show that, whereas TNFα induces the stimulation of autophagy in Ewing sarcoma cells lacking NF-κB activity, it does not activate this process in Ewing sarcoma NF-κB-competent cells. Similar results were observed in another clone of Ewing sarcoma cells and NB4 cells carrying a repressor for NF-κB activation as well as in MCF7 cells following inhibition of p65 expression by using specific siRNA. These findings support the conclusion that the NF-κB-dependent inhibition of autophagy may be a general cellular response.

Although the implication of autophagy in nonapoptotic programmed cell death, known as autophagic cell death (54–56), has been pointed out in several studies, its contribution to apoptosis is less clear. Here, we show that siRNA-mediated knockdown of autophagy-related genes reduces TNFα-induced apoptosis in cells lacking NF-κB activation. These findings contradicted by results showing that autophagy is an antiapoptotic mechanism under certain stress conditions (25, 30, 57). Thus, depending on cellular context, autophagy may have pro-apoptotic or antiapoptotic functions. The molecular mechanisms that determine the switch between these two responses remain to be elucidated.

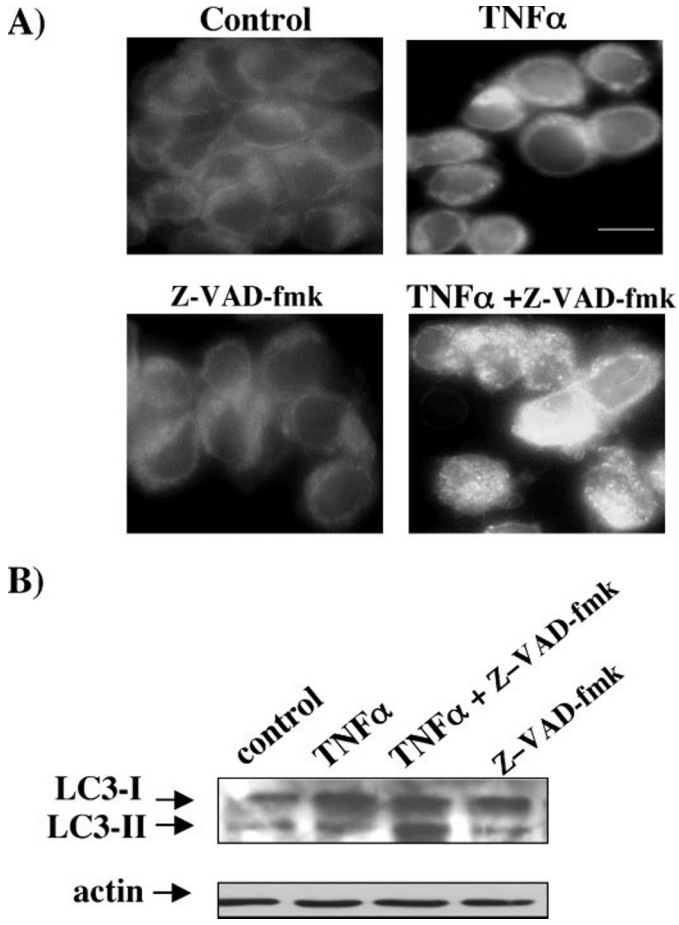

FIGURE 7. **Effect of caspase inhibition on TNFα-induced autophagy in EW7MAD1 cells.** EW7MAD1 cells were first incubated for 2 h with Z-VAD-fmk (50 μM) and then treated for 8 h with TNFα The *bar* represents 6 μm. *A*, cells were subjected to MDC staining before analysis by fluorescence microscopy. *B*, cellular extracts were prepared for Western blotting analysis of LC3-II expression. Results shown in *A* and *B* are representative of three independent experiments.

The role of caspase in the modulation of autophagy activity has been pointed out in few recent studies (26, 32). Here, we found that the inhibition of caspase activation by Z-VAD-fmk, which totally inhibits TNFα-induced apoptosis, enhances TNFα-mediated stimulation of autophagy in cells lacking NF-κB activation. This suggests that the activation of caspases can in turn control the initial autophagic activity. The negative regulation of autophagic activity by caspases has also been reported by Xue *et al.* (58), who showed that blockade of caspase activities induces an autophagy-related sequestration of mitochondria in nerve growth factor-deprived neuroblastoma cells. Recently, another report (32) demonstrates that autophagy-related cell death is induced by caspase 8 inactivation. Hence, our findings, together with these results, support the notion that autophagy and apoptosis may regulate each other.

We and others have previously shown that impairment of NF-κB activation results in accumulation of ROS in several cell lines in response to distinct activators of NF-κB (41, 48, 49). The role of ROS in autophagy stimulation has been shown by using oxidative stress conditions, such as treatment of neuroblastoma cells with dopamine (57), hyperoxia (59), and in Syrian hamster Harderian gland, a physiological model of oxidative stress (60). Nevertheless, direct evidence that ROS induces autophagy has been lacking. In the present report, we demonstrate that ROS participate in TNFα-induced stimulation of autophagy in cells carrying a repressor of NF-κB and that direct addition of exogenous H_2O_2 to NF-κB-competent cells is also able to induce autophagy. Furthermore, we found that TNFα and H_2O_2 rapidly induce Beclin 1 expression in EW7MAD1 cells and EW7PC cells, respectively. In both cases, the increase in Beclin 1 expression precedes the accumulation of autophagic vacuoles. Moreover, the antioxidants BHA and BNP markedly prevent the increase in Beclin 1 expression and autophagy, suggesting that ROS are involved in these processes. It has been reported that the level of expression of Bcl-2 plays a role in the regulation of autophagy through its interaction with Beclin 1 (44, 61). Hence, our observation that TNFα mediates down-regulation of Bcl-2 protein in cells lacking NF-κB activation argues for a possible mechanism by which autophagy may be stimulated in these cells.

The mTOR pathway has been shown to regulate autophagy negatively (19, 43). Here, we provide evidence that TNFα upregulates mTOR activity in an NF-κB-dependent manner, since this activity is induced in TNFα-treated NF-κB-competent cells and, inversely, impaired in TNFα-treated cells lacking NF-κB activity. These results are consistent with the opposite autophagic capacities observed in these two cell lines after treatment with TNFα. Nevertheless, the molecular mechanisms by which NF-κB activity regulates mTOR activity require more extensive investigations.

In conclusion, we demonstrate that NF-κB-mediated repression of autophagy may constitute a novel antiapoptotic mechanism of this transcription factor. This suggests that activation of autophagy is a potential way of bypassing the resistance of cancer cells to anti-cancer agents that activate NF-κB.

Acknowledgments—We thank Dr. O. Delattre and Prof. G. Lenoir for providing the Ewing sarcoma cells. We are grateful to Dr. William A. Dunn, Jr., Dr. Eiki Kominami, and Dr. Tamotsu Yoshimori for providing reagents used in this study. We are grateful to Claudine Deloménie (Plateforme Transcriptome-Protéome, IFR 141 ITFM, Faculté de Pharmacie, Université Paris-sud 11, France) for help in real time quantitative reverse transcription-PCR experiments.

Addendum—During review of this manuscript, the role of ROS in the induction of autophagy in macrophages was reported (62).

REFERENCES

1. Mayo, M. W., and Baldwin, A. S. (2000) *Biochim. Biophys. Acta* **1470,** M55–M62
2. Bharti, A. C., and Aggarwal, B. B. (2002) *Biochem. Pharmacol.* **64,** 883–888
3. Luo, J. L., Kamata, H., and Karin, M. (2005) *J. Clin. Invest.* **115,** 2625–2632
4. Nakanishi, C., and Toi, M. (2005) *Nat. Rev. Cancer* **5,** 297–309
5. Baeuerle, P. A., and Baltimore, D. (1996) *Cell* **87,** 13–20
6. Karin, M., and Lin, A. (2002) *Nat. Immunol.* **3,** 221–227
7. Barkett, M., and Gilmore, T. D. (1999) *Oncogene* **18,** 6910–6924
8. Baldwin, A. S., Jr. (1996) *Annu. Rev. Immunol.* **14,** 649–683
9. Bours, V., Dejardin, E., Goujon-Letawe, F., Merville, M. P., and Castronovo, V. (1994) *Biochem. Pharmacol.* **47,** 145–149

10. Orlowski, R. Z., and Baldwin, A. S., Jr. (2002) *Trends Mol. Med.* **8,** 385–389
11. Ogier-Denis, E., and Codogno, P. (2003) *Biochim. Biophys. Acta* **1603,** 113–128
12. Alva, A. S., Gultekin, S. H., and Baehrecke, E. H. (2004) *Cell Death Differ.* **11,** 1046–1048
13. Klionsky, D. J., and Emr, S. D. (2000) *Science* **290,** 1717–1721
14. Seglen, P. O., and Bohley, P. (1992) *Experientia* **48,** 158–172
15. Tsukada, M., and Ohsumi, Y. (1993) *FEBS Lett.* **333,** 169–174
16. Thumm, M., Egner, R., Koch, B., Schlumpberger, M., Straub, M., Veenhuis, M., and Wolf, D. H. (1994) *FEBS Lett.* **349,** 275–280
17. Klionsky, D. J., Cregg, J. M., Dunn, W. A., Jr., Emr, S. D., Sakai, Y., Sandoval, I. V., Sibirny, A., Subramani, S., Thumm, M., Veenhuis, M., and Ohsumi, Y. (2003) *Dev. Cell* **5,** 539–545
18. Ohsumi, Y. (2001) *Nat. Rev. Mol. Cell. Biol.* **2,** 211–216
19. Kihara, A., Noda, T., Ishihara, N., and Ohsumi, Y. (2001) *J. Cell Biol.* **152,** 519–530
20. Liang, X. H., Jackson, S., Seaman, M., Brown, K., Kempkes, B., Hibshoosh, H., and Levine, B. (1999) *Nature* **402,** 672–676
21. Kroemer, G., and Jaattela, M. (2005) *Nat. Rev. Cancer* **5,** 886–897
22. Baehrecke, E. H. (2005) *Nat. Rev. Mol. Cell. Biol.* **6,** 505–510
23. Kuma, A., Hatano, M., Matsui, M., Yamamoto, A., Nakaya, H., Yoshimori, T., Ohsumi, Y., Tokuhisa, T., and Mizushima, N. (2004) *Nature* **432,** 1032–1036
24. Lum, J. J., Bauer, D. E., Kong, M., Harris, M. H., Li, C., Lindsten, T., and Thompson, C. B. (2005) *Cell* **120,** 237–248
25. Boya, P., Gonzalez-Polo, R. A., Casares, N., Perfettini, J. L., Dessen, P., Larochette, N., Metivier, D., Meley, D., Souquere, S., Yoshimori, T., Pierron, G., Codogno, P., and Kroemer, G. (2005) *Mol. Cell. Biol.* **25,** 1025–1040
26. Martin, D. N., and Baehrecke, E. H. (2004) *Development* **131,** 275–284
27. Kondo, Y., Kanzawa, T., Sawaya, R., and Kondo, S. (2005) *Nat. Rev. Cancer* **5,** 726–734
28. Jaattela, M. (2004) *Oncogene* **23,** 2746–2756
29. Mills, K. R., Reginato, M., Debnath, J., Queenan, B., and Brugge, J. S. (2004) *Proc. Natl. Acad. Sci. U. S. A.* **101,** 3438–3443
30. Jia, L., Dourmashkin, R. R., Allen, P. D., Gray, A. B., Newland, A. C., and Kelsey, S. M. (1997) *Br. J. Haematol.* **98,** 673–685
31. Lemasters, J. J., Nieminen, A. L., Qian, T., Trost, L. C., Elmore, S. P., Nishimura, Y., Crowe, R. A., Cascio, W. E., Bradham, C. A., Brenner, D. A., and Herman, B. (1998) *Biochim. Biophys. Acta* **1366,** 177–196
32. Yu, L., Alva, A., Su, H., Dutt, P., Freundt, E., Welsh, S., Baehrecke, E. H., and Lenardo, M. J. (2004) *Science* **304,** 1500–1502
33. Pyo, J. O., Jang, M. H., Kwon, Y. K., Lee, H. J., Jun, J. I., Woo, H. N., Cho, D. H., Choi, B., Lee, H., Kim, J. H., Mizushima, N., Oshumi, Y., and Jung, Y. K. (2005) *J. Biol. Chem.* **280,** 20722–20729
34. Javelaud, D., Wietzerbin, J., Delattre, O., and Besancon, F. (2000) *Oncogene* **19,** 61–68
35. Mathieu, J., Giraudier, S., Lanotte, M., and Besancon, F. (2005) *Oncogene* **24,** 7145–7155
36. Biederbick, A., Kern, H. F., and Elsasser, H. P. (1995) *Eur. J. Cell Biol.* **66,** 3–14
37. Pattingre, S., Petiot, A., and Codogno, P. (2004) *Methods Enzymol.* **390,** 17–31
38. Lavieu, G., Scarlatti, F., Sala, G., Carpentier, S., Levade, T., Ghidoni, R., Botti, J., and Codogno, P. (2006) *J. Biol. Chem.* **281,** 8518–8527
39. Zhou, A., Scoggin, S., Gaynor, R. B., and Williams, N. S. (2003) *Oncogene* **22,** 2054–2064
40. Kabeya, Y., Mizushima, N., Yamamoto, A., Oshitani-Okamoto, S., Ohsumi, Y., and Yoshimori, T. (2004) *J. Cell Sci.* **117,** 2805–2812
41. Djavaheri-Mergny, M., Javelaud, D., Wietzerbin, J., and Besancon, F. (2004) *FEBS Lett.* **578,** 111–115
42. Blommaart, E. F., Luiken, J. J., Blommaart, P. J., van Woerkom, G. M., and Meijer, A. J. (1995) *J. Biol. Chem.* **270,** 2320–2326
43. Noda, T., and Ohsumi, Y. (1998) *J. Biol. Chem.* **273,** 3963–3966
44. Pattingre, S., Tassa, A., Qu, X., Garuti, R., Liang, X. H., Mizushima, N., Packer, M., Schneider, M. D., and Levine, B. (2005) *Cell* **122,** 927–939
45. Ollinger, K., and Roberg, K. (1997) *J. Biol. Chem.* **272,** 23707–23711
46. Kucharczak, J., Simmons, M. J., Fan, Y., and Gelinas, C. (2003) *Oncogene* **22,** 8961–8982
47. Chen, C., Edelstein, L. C., and Gelinas, C. (2000) *Mol. Cell. Biol.* **20,** 2687–2695
48. Sakon, S., Xue, X., Takekawa, M., Sasazuki, T., Okazaki, T., Kojima, Y., Piao, J. H., Yagita, H., Okumura, K., Doi, T., and Nakano, H. (2003) *EMBO J.* **22,** 3898–3909
49. Kamata, H., Honda, S., Maeda, S., Chang, L., Hirata, H., and Karin, M. (2005) *Cell* **120,** 649–661
50. Iwanaga, M., Mori, K., Iida, T., Urata, Y., Matsuo, T., Yasunaga, A., Shibata, S., and Kondo, T. (1998) *Free Radic. Biol. Med.* **24,** 1256–1268
51. Bernard, D., Monte, D., Vandenbunder, B., and Abbadie, C. (2002) *Oncogene* **21,** 4392–4402
52. Brouard, S., Berberat, P. O., Tobiasch, E., Seldon, M. P., Bach, F. H., and Soares, M. P. (2002) *J. Biol. Chem.* **277,** 17950–17961
53. Pham, C. G., Bubici, C., Zazzeroni, F., Papa, S., Jones, J., Alvarez, K., Jayawardena, S., De Smaele, E., Cong, R., Beaumont, C., Torti, F. M., Torti, S. V., and Franzoso, G. (2004) *Cell* **119,** 529–542
54. Clarke, P. G. (1990) *Anat. Embryol.* (*Berl.*) **181,** 195–213
55. Lockshin, R. A., and Zakeri, Z. (2004) *Oncogene* **23,** 2766–2773
56. Levine, B., and Yuan, J. (2005) *J. Clin. Invest.* **115,** 2679–2688
57. Gomez-Santos, C., Ferrer, I., Santidrian, A. F., Barrachina, M., Gil, J., and Ambrosio, S. (2003) *J. Neurosci. Res.* **73,** 341–350
58. Xue, L., Fletcher, G. C., and Tolkovsky, A. M. (2001) *Curr. Biol.* **11,** 361–365
59. Zheng, L., Roberg, K., Jerhammar, F., Marcusson, J., and Terman, A. (2005) *Neurosci. Lett.* **394,** 184–189
60. Tomas-Zapico, C., Caballero, B., Sierra, V., Vega-Naredo, I., Alvarez-Garcia, O., Tolivia, D., Rodriguez-Colunga, M. J., and Coto-Montes, A. (2005) *FASEB J.* **19,** 2066–2068
61. Saeki, K., Yuo, A., Okuma, E., Yazaki, Y., Susin, S. A., Kroemer, G., and Takaku, F. (2000) *Cell Death Differ.* **7,** 1263–1269
62. Xu, Y., Kim, S. O., Li, Y., and Han, J. (2006) *J. Biol. Chem.* **281,** 19179–19187